Plasmon-assisted delivery of single nano-objects in an optical *hot-spot*

Christopher M. Galloway [1], Mark P. Kreuzer [1], Srdjan S. Aćimović [1], Giorgio Volpe [1], Manuel Correia [2], Steffen B. Petersen [4], Maria Teresa Neves-Petersen [3, *], Romain Quidant [1, 5, *]

[1] ICFO - Institut de Ciencies Fotoniques, Mediterranean Technology Park, 08860 Castelldefels (Barcelona), Spain

[2] Department of Physics and Nanotechnology, Aalborg University, Skjernvej 4A. DK-9220, Aalborg, Denmark

[3] International Iberian Nanotechnology Laboratory (INL), P-4715-310 Braga, Portugal

[4] NanoBiotechnology Group, Department of Health Science and Technology, Aalborg University, Fredrik Bajers vej 7, DK-9220, Aalborg, Denmark

[5] ICREA - Institució Catalana de Recerca i Estudis Avançats, Barcelona, Spain

* teresa.petersen@inl.int , romain.quidant@icfo.es

Fully exploiting the capability of nano-optics to enhance light-matter interaction on the nanoscale is conditioned by bringing the nano-object to interrogate within the minuscule volume where the field is concentrated. There currently exist several approaches to control the immobilization of nano-objects but they all involve a cumbersome delivery step and require prior knowledge of the *hot spot* location[1,2,3,4,5,6]. Herein, we present a novel technique in which the enhanced local field in the *hot spot* is the driving mechanism which triggers the binding of proteins via three-photon absorption. This way, we demonstrate exclusive immobilization of nanoscale amounts of BSA molecules into the nanometer-sized gap of plasmonic dimers. The immobilized proteins can then act as a scaffold to subsequently attach an additional nanoscale object such as a molecule or a nanocrystal. This universal

technique is envisioned to benefit a wide range of nano-optical functionalities including biosensing[7,8,9,10,11,12], enhanced spectroscopy like SERS[13,14] or SEIRA[15] as well as quantum optics[1,2,6].

Recent advances in nano-optics and especially in plasmonics offer a unique capability to concentrate light fields well below the limit of diffraction. While nanoscale control of light opens up a huge potential that could benefit many different fields of science, its full exploitation raises major technical challenges. Indeed, the more confined is the optical field the more critical and challenging becomes the positioning of the specimen as a small spatial shift translates into a strong change of the interaction strength. With the aim to achieve a deterministic control of enhanced light-matter interaction in an optical *hot spot,* researchers have recently proposed strategies to position few to single quantum emitters at a predefined location of plasmonic nanostructures. A first family of techniques consists in using scanning probes or optical tweezers to pick up one specimen and move it to its final destination[16,17,18]. Although accurate, these approaches are tedious and not scalable to a large number of structures. Alternatively, double-step lithography combined with surface chemistry was successfully used to immobilize few to single quantum dots at predefined locations of large arrays of optical antennas[1,2,6]. While the first lithography defines the plasmonic pattern, the second one opens binding sites where the quantum dots subsequently attach. Again such a process is cumbersome and its precision limited by the accuracy with which the sample is aligned for the second lithography, typically of the order of 20nm. More

importantly, all these approaches fully rely on a prior knowledge of the *hot spot* location, which is extremely sensitive to any morphological defect or irregularities of the optical nanostructure. The photochemical approach we propose here addresses the limitations of existing strategies by building upon the actual (and not the expected) near field optical response of the fabricated nanostructures.

Our strategy relies on light-assisted molecular immobilization (LAMI)[19,20,21], in which proteins can be immobilized onto a thiol-reactive surface [22,23,24], by absorption of UV photons. LAMI technology exploits an inherent natural property of proteins and peptides whereby a disulphide bridge is disrupted upon absorption of UV photons by the nearby aromatic amino acids. The created thiol groups are subsequently used to immobilise the protein or peptide to a substrate or nanoparticle. This photonic protein immobilization technology has led to the development of microarrays of active biosensors and biofunctionalization of thiol reactive nanoparticles, aimed at drug delivery systems[21,25]. LAMI has so far been used to create high-density protein arrays with a resolution that is only restricted by the focussing ability of the light source, typically limited by diffraction to approximately half the wavelength of light. Therefore, the best-case scenario allowed protein spots of the order of a few hundred nanometers to be manufactured. The use of plasmonics could enable the immobilization of much smaller amounts of molecules by capitalizing on the capability of metallic nanostructures to concentrate light on the sub-wavelength scale. While the aromatic residue of proteins features an absorption peak centred at around 275nm (274nm for

tyrosine and 278nm for tryptophan), gold nanostructures are usually resonant in the near-infrared region of the spectrum. To compensate for this energy mismatch, we employ absorption of multiple infrared photons from the optical near field of the nanostructures. In addition, LAMI based on multiphoton absorption[26,27,28] is expected to further improve the spatial resolution of the immobilization by restricting the photochemical reaction to the region of most intense optical fields[29].

In the present experimental implementation, periodic arrays of gold dimers were fabricated on glass by using standard e-beam lithography. The dimensions of the two identical cylinders forming the dimers were tuned to achieve a resonance centered ca. 700nm in air. Scanning Electron Microscopy (SEM) shows an average gap size of 20 $\pm$ 5nm in which most of the plasmonic field is expected to be confined upon illumination polarized along the dimer longitudinal axis. As a result of the protein coverage, which is achieved by evaporation, the resonance of the dimers shift to ca. 800nm, thus enabling three-photon absorption upon illumination with a pulsed Titanium:Sapphire laser (set at 810nm) to initiate the LAMI process.

Figure 1 demonstrates how the spatial distribution of immobilized proteins varies with the laser power (illumination focus of 12µm). Arrays of gold dimers were coated with Alexa-488 labeled bovine serum albumin (BSA) and exposed at differing powers before being cleaned of all unbound BSA (see supplementary information for experimental details).

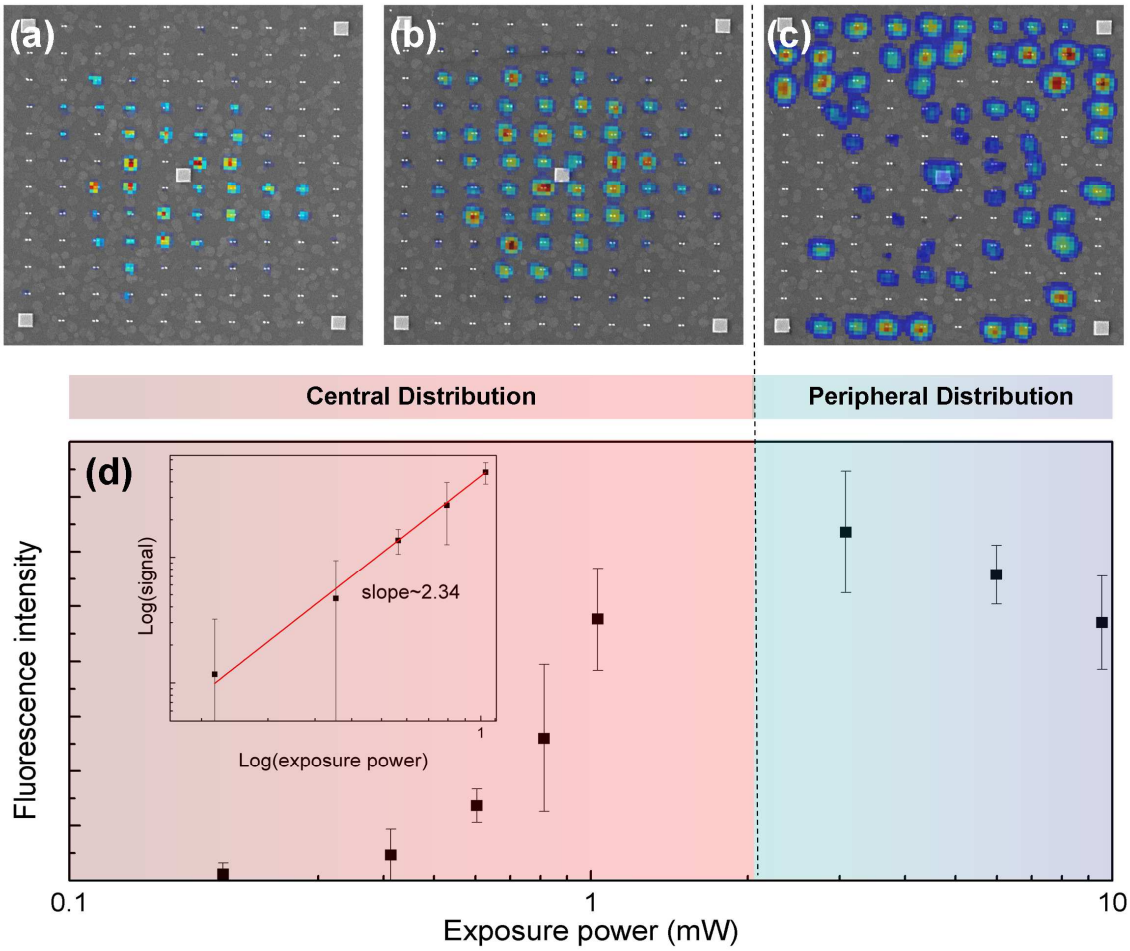

Figure 1: **Evolution of the spatial distribution of immobilized proteins as a function of the illumination power**: SEM images of three arrays illuminated at powers of (a) 600 µW (b) 1 mW and (c) 10 mW are superimposed with their corresponding fluorescence maps (note: the color scale is not constant) with red representing strong fluorescence and blue representing weak fluorescence. The dimers are separated by 1µm in both directions and have dimensions as explained in the supplementary information. (d) Plot of the dependence with exposure power of the average fluorescence of the 10 dimers with the largest fluorescent signal. The error bars represent the spread in those 10 values. Inset in (d) is a logarithmic plot of the power dependence of the average fluorescence for a central distribution demonstrating the multi-photon mechanism.

Three of the arrays imaged by SEM are shown in figure 1 (a)-(c) and overlaid with their corresponding fluorescence maps. The location of the fluorescence demonstrates how

the proteins are arranged on the array surface while its intensity provides qualitative information on the local density of protein binding. Two spatial regimes are clearly apparent; *central immobilization* (red region of Fig. 1(d)), in which the dimers with the largest fluorescence are located in the center of the array, and a *peripheral immobilization* (blue region of Fig. 1(d)) where the inner structures show little or no fluorescence and the largest fluorescence come from the dimers at the periphery of the array. This phenomenon is due to the Gaussian intensity profile of the IR beam used to illuminate the arrays such that the central dimers experience the largest laser intensity. However, if the local intensity becomes too high, protein immobilization will cease resulting in the ring-like peripheral pattern. We postulate that the main contributing factor here is heating of the gold to temperatures that lead to the breaking of the thiol bond that anchors the protein to the gold. For those maps with central immobilization (those where the central structures are not over-exposed), the integrated fluorescence intensity (see supplementary information) varies non-linearly with power as demonstrated from the inset logarithmic plot in fig. 1(d). A slope of ca. 2.34 is achieved demonstrating that the immobilization involves the absorption of more than two infrared photons.

In order to verify that the protein binding is triggered by the enhanced plasmonic fields produced by the dimer at its localized surface plasmon resonance (LSPR), arrays with different resonant wavelengths were exposed under identical excitation conditions (see supplementary information). The array with a resonance closest to the exposing

wavelength, set at 810nm (fig. 2(b)), shows a larger fluorescence signal as compared to the arrays whose resonance is shifted (see fig. 2(d) for the extinction spectra). It is interesting to note that the array with the longest resonance wavelength has the largest surface area of gold but shows the least amount of fluorescence. This confirms that the optical near field governs the proteins immobilization independently of the geometry of the gold structure.

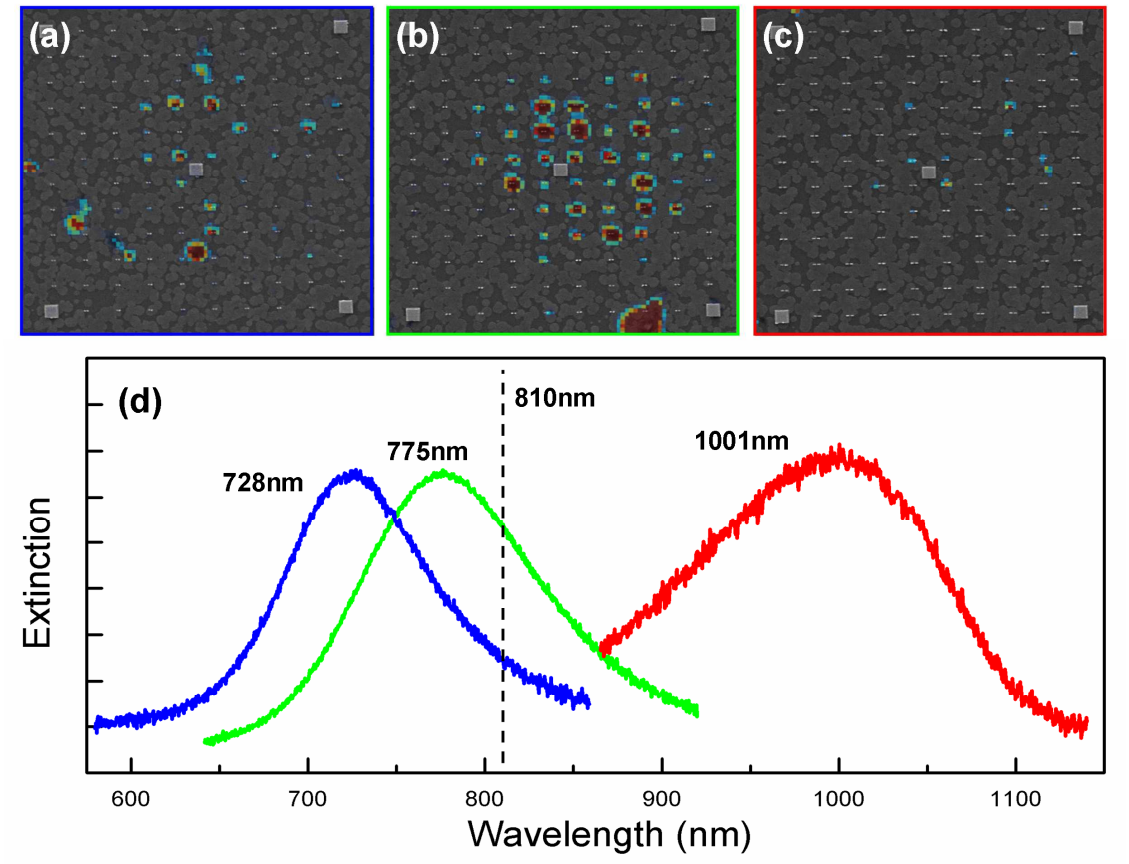

Figure 2: **Effect of the plasmon resonance on protein immobilization**. SEM images of arrays with resonance wavelengths (when coated with BSA) of (a) 728 nm, (b) 775 nm and (c) 1001 nm are superimposed with their fluorescence maps (the color scale is kept constant). (d) Extinction spectra for the 3 different dimer arrays. The dashed line at 810nm represents the wavelength at which the structures were illuminated.

The susceptibility of the immobilization to the resonant optical properties of the gold antenna suggests that under the right conditions, proteins can be exclusively bound to the regions of highest field enhancement. However, due to the small dimensions of the plasmonic structure, techniques other than conventional confocal microscopy need to be utilized to determine the spatial distribution of proteins on the gold surface. Fortunately, the protein localization can be observed as a dark "clouding" using SEM microscopy[30]. In fig. 3, fig. 3(a) is an unexposed array, while fig. 3(b) was exposed with 1mW (see supplementary information for details on visualizing proteins clouds). For convenience, these arrays feature a higher density (lower pitch) so that the illumination seen by each structure is as homogeneous as possible. Compared to the non-exposed array, there is substantially more clouding in the exposed case, particularly in the gap region of the structures. Furthermore, there is very little sign of clouding at other locations of the gold surface. To complement this initial visual effect, we exploit the intrinsic sensitivity of LSPR resonances to the binding of proteins at the gold surface. The shift in the resonance peak depends on both the number of proteins and their location [3,31]. In particular, it will be more pronounced when the molecules overlap with the regions where the near field is the most concentrated. Fig. 3(c) displays the evolution in the dimers resonance as the power of the exposing beam increases.

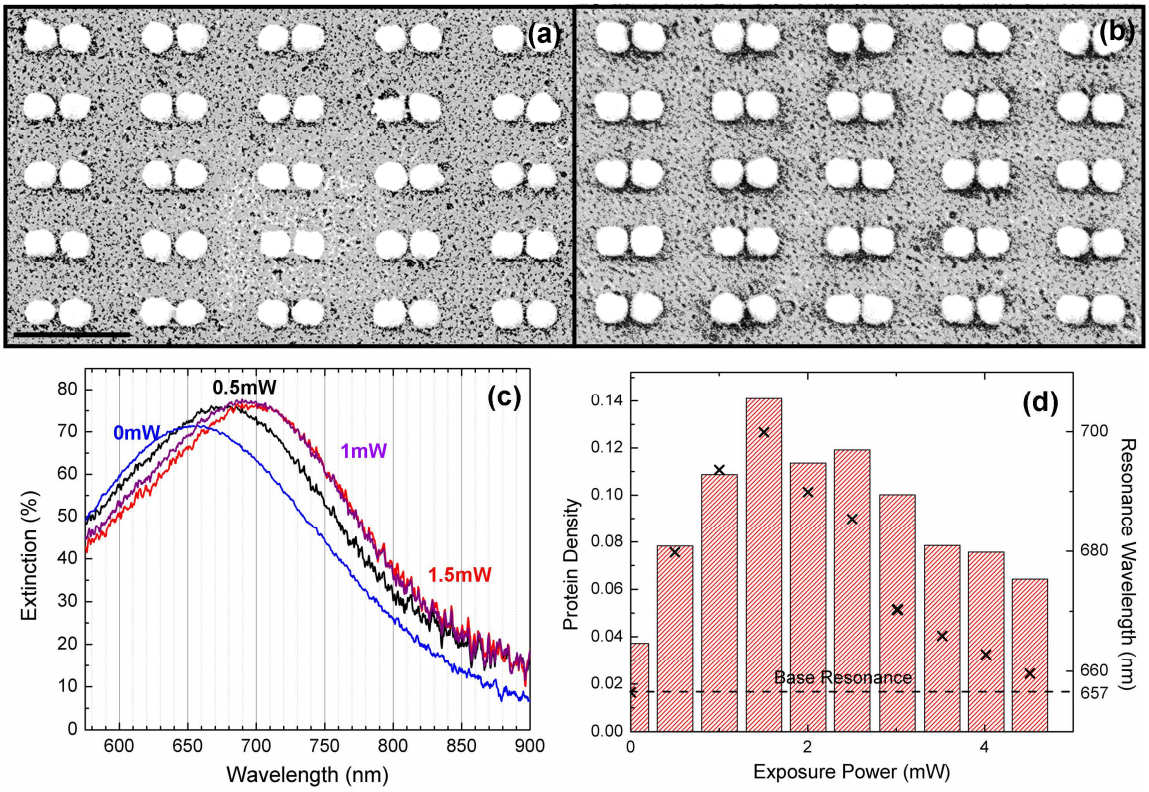

Figure 3: **Monitoring of molecule binding in the dimers gap**: Processed SEM images of a set of 5x5 gold dimers (scale bar=500nm) (a) unexposed and (b) after exposure at 1mW. (c) Shift of the extinction spectrum of the arrays for increasing exposure powers. (d) Evolution with the exposure power of the protein density extracted from SEM imaging (bars) and the peak resonance wavelengths (crosses).

Upon increasing incident power, the LSPR wavelength rapidly shifts from 657m to a maximum of 700nm for a power of 1.5mW before decreasing back to the initial level. The protein density extracted from SEM imaging is well correlated to the resonance shift, featuring a similar resonant behavior (fig. 3(d)). Interestingly though, for powers larger than 1.5mW the decay is slower, indicating that the immobilized proteins have a decreasing influence on the dimer resonance. For example, the protein density at 0.5mW and 3.5mW are very similar, however, the resonance shift at 0.5mW is approximately twice that at 3.5mW. This confirms that at low powers, the proteins are

mainly located in the gap region of the structures where they have a larger influence on the LSPR wavelength[31].

At this stage, we propose to exploit the proteins immobilized in the region of most intense field as a scaffold to attach any additional nano-objects of interest. The latter would then be automatically located at the position at which the interaction with the plasmonic field is optimum. To demonstrate this we chose to modify the immobilized BSA protein with biotin with 0.5 mW and then allow streptavidin-coated gold colloids to interact with the system[32,33] (see fig. 4(a) and supplementary information for more details). The choice of gold colloids over quantum emitters such as a quantum dot is because the colloids can be easily imaged via SEM. Fig. 4(b) and (c) show two high-resolution examples in which a highly symmetric dimer has bound a single 20nm colloid very close to the gap center. However, most of nanofabricated structures feature morphological imperfections that lead to a *hot spot* that is not exactly located in the very center of the gap between the two gold particles forming the dimer. The strength of our approach is that it automatically accounts for these slight variations such that the hosting protein scaffold builds where the field is actually concentrated. Despite the unique fine geometrical features of each of the dimers shown in fig. 4(d), the gold colloid attaches in or very close to the region of smallest gap. Such self-alignment makes the process directly transposable to more complex architectures without any need for a prior knowledge of the *hot spot* location.

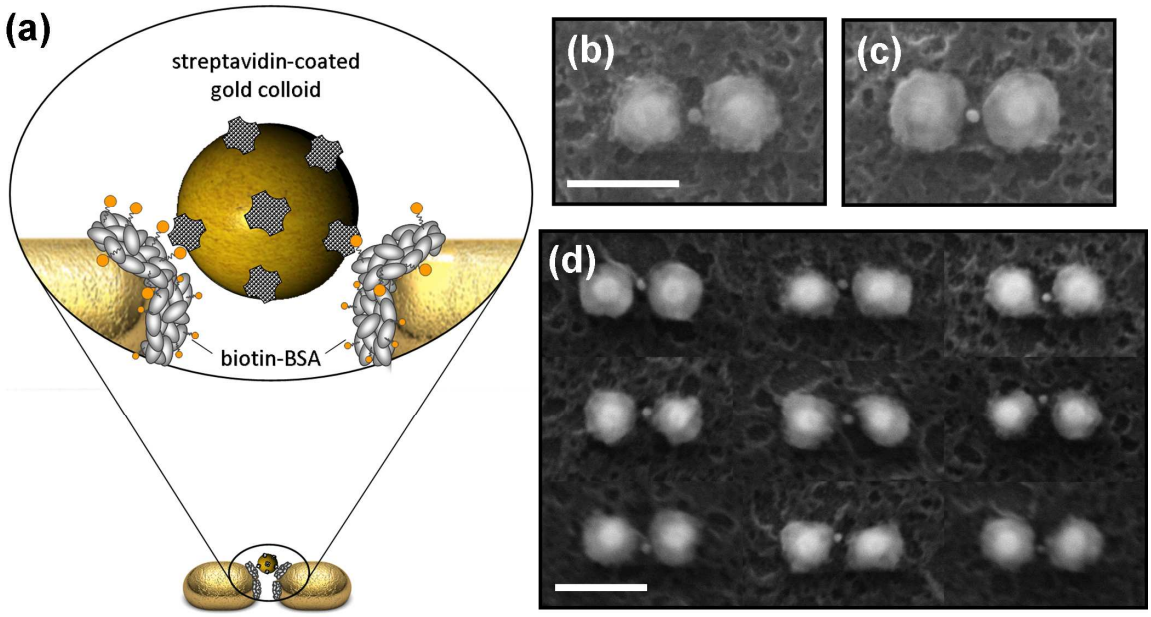

Figure 4: **Immobilization of single nano-object in the gap of gold dimers**: (a) Schematic of the chemical modification used to bind a gold colloid to the immobilized protein. (b) and (c) SEM images showing binding of a single gold nanoparticle in the gap of homogeneous gold dimers. (d) Series of SEM images that illustrates self-alignment of the gold colloid in the hot spot despite the morphological irregularities of the hosting dimers (scale bar= 150nm).

Beyond the present proof of concept, we envision this approach to benefit a wide range of research areas involving the interaction of an inhomogeneous optical near field with tiny amounts of matter. This includes plasmon-enhanced optical spectroscopy techniques such as surface-enhanced Raman spectroscopy (SERS) and infrared absorption spectroscopy (SEIRA) in which the magnitude of the signal directly depends on analyte/*hot spot* overlap. Also our technique may improve the sensitivity in biosensing, whereby the precise positioning of receptors, in the most sensitive region, remains both allusive and technologically challenging[3]. Finally, it may also be useful in quantum optics where the strong coupling between quantum emitters and strongly confined optical modes is a crucial condition to fulfil in many quantum functionalities.

Acknowledgements

This work was partially supported by the Spanish Ministry of Sciences under grants FIS2010–14834 and CSD2007–046-NanoLight.es, the European Community's Seventh Framework Program under grant ERC-Plasmolight (259196), and Fundació privada CELLEX.

1. Bermúdez Ureña, E. *et al*. Excitation enhancement of a quantum dot coupled to a plasmonic antenna. *Adv. Mater*. **24**, OP314-OP320 (2012).

2. Curto, A. G. *et al*. Unidirectional emission of a quantum dot coupled to a nanoantenna. *Science* **329**, 930-933 (2010).

3. Feuz, L., Jonsson, M. P. & Höök, F. Material-selective surface chemistry for nanoplasmonic sensors: Optimizing sensitivity and controlling binding to local hot spots. *Nano Lett*. **12**, 873-879 (2012).

4. Kramer, R. K. *et al*. Positioning of quantum dots on metallic nanostructures. *Nanotechnology* **21**, 145307 (2010).

5. Pfeiffer, M. *et al*. Positioning plasmonic nanostructures on single quantum emitters. *Phys*. *Status Solidi B* **249**, 678-686 (2012).

6. Dregely, D. *et al*. Plasmonic antennas, positioning, and coupling of individual quantum systems. *Phys*. *Status Solidi B* **249**, 666–677 (2012).

7. Anker, J. N. *et al*. Biosensing with plasmonic nanosensors. *Nature Mater*. **7**, 442-453 (2008).

8. Chen, S., Svedendahl, M., Käll, M., Gunnarsson, L. & Dmitriev, A. Ultrahigh sensitivity made simple: Nanoplasmonic label-free biosensing with an extremely low limit-of-detection for bacterial and cancer diagnostics. *Nanotechnology* **20**, 434015 (2009).

9. Hoa, X. D., Kirk, A.G. & Tabrizian, M. Towards integrated and sensitive surface plasmon resonance biosensors: A review of recent progress. *Biosens*. *Bioelectron*. **23**, 151-160 (2007).

10. Kabashin, A. V. *et al*. Plasmonic nanorod metamaterials for biosensing. *Nature Mater*. **8**, 867-871 (2009).

11. Hendry, E. *et al*. Ultrasensitive detection and characterization of biomolecules using superchiral fields. *Nature Nanotechnol*. **5**, 783-787 (2010).

12. Lee, J., Hernandez, P., Lee, J. Govorov, A. O. & Kotov, N. A. Exciton–plasmon interactions in molecular spring assemblies of nanowires and wavelength-based protein detection. *Nature Mater*. **6**, 291-295 (2007).

13. De Angelis, F. *et al*. Breaking the diffusion limit with super-hydrophobic delivery of molecules to plasmonic nanofocusing SERS structures. *Nature Photon*. **5**, 682-687 (2011).

14. Hu, M. *et al*. Gold nanofingers for molecule trapping and detection. *J*. *Am*. *Chem*. *Soc*. **132**, 12820-12822 (2010).

15. Adato, R. *et al*. Ultra-sensitive vibrational spectroscopy of protein monolayers with plasmonic nanoantenna arrays. *Proc*. *Natl*. *Acad*. *Sci*. **106**, 19227-19232 (2009).

16. Kühn, S., Håkanson, U., Rogobete, L. & Sandoghdar, V. Enhancement of single-molecule fluorescence using a gold nanoparticle as an optical nanoantenna. *Phys*. *Rev. Lett*. **97**, 017402 (2006).

17. Schietinger, S., Barth, M., Aichele, T. & Benson, O. Plasmon-enhanced single photon emission from a nanoassembled metal-diamond hybrid structure at room temperature, *Nano Lett*. **9**, 1694-1698 (2009).

18. Geiselmann, M. *et al*. Three-dimensional optical manipulation of a single electron spin. *Nature Nanotechnol*. **8**, 175-179 (2013).

19. Snabe, T., Røder, G. A., Neves-Petersen, M. T., Buusb, S. & Petersen, S. B. Oriented coupling of major histocompatibility complex (MHC) to sensor surfaces using light assisted immobilisation technology. *Biosens*. *Bioelectron*. **21**, 1553–1559 (2006).

20. Neves-Petersen, M. T., Snabe, T., Klitgaard, S., Duroux, M. & Petersen, S. P. Photonic activation of disulfide bridges achieves oriented protein immobilization on biosensor surfaces. *Protein Sci*. **15**, 343-351 (2006).

21. Duroux, M. *et al*. Light-induced immobilisation of biomolecules as an attractive alternative to microdroplet dispensing-based arraying technologies. *Proteomics* **7**, 3491-3499 (2007).

22. Collioud, A., Clémence, J.-F., Sänger, M. & Sigrist, H. Oriented and covalent immobilization of target molecules to solid supports: Synthesis and application of a

light-activatable and thiol-reactive cross-linking reagent. *Bioconjugate Chem*. **4**, 528-536 (1993).

23. Jonkheijm, P., Weinrich, D., Schröder, H., Niemeyer, C. M. & Waldmann, H. Chemical strategies for generating protein biochips. *Angew*. *Chem*. *Int*. *Ed*. **47**, 9618-9647 (2008).

24. Sigrist, H. *et al*. Surface immobilization of biomolecules by light. *Opt*. *Eng*. **34**, 2339-2348 (1995).

25. Parracino, A. *et al*. Photonic immobilization of BSA for nanobiomedical applications: Creation of high density microarrays and superparamagnetic bioconjugates. *Biotechnol*. *Bioeng*. **108**, 999-1010 (2011).

26. Gryczynski, I., Malak, H. & Lakowicz, J. R. Three-photon excitation of a tryptophan derivative using a fs-Ti : sapphire laser. *Biospectroscopy* **2**, 9-15 (1996).

27. Gryczynski, I. *et al*. Fluorescence spectral properties of troponin C mutant F22W with one-, two-, and three-photon excitation. *Biophys*. *J*. **71**, 3448-3453 (1996).

28. Maiti, S., Shear, J. B., Williams, R. M., Zipfel, W. R. & Webb, W. W. Measuring serotonin distribution in live cells with Three-Photon Excitation. *Science* **275**, 530-532 (1997).

29. Volpe, G., Noack, M., Aćimović, S. S., Reinhardt, C. & Quidant, R. Near-field mapping of plasmonic antennas by multiphoton absorption in poly(methyl methacrylate). *Nano Lett*. **12**, 4864−4868 (2012).

30. López, G. P., Biebuyck, H. A., Härter, R., Kumar, A. & Whitesides, G. M. Fabrication and imaging of two-dimensional patterns of proteins adsorbed on self-assembled monolayers by scanning electron microscopy. *J*. *Am*. *Chem*. *Soc*. **115**, 10774-10781 (1993).

31. Aćimović, S. S., Kreuzer, M. P., González, M. U., & Quidant, R. Plasmon near-field coupling in Metal dimers as a step toward single-molecule sensing. *Nano Lett*. **3**, 1231-1237 (2009).

32. Caswell, K. K., Wilson, J. N., Bunz, U. H. F., & Murphy, C. J. Preferential end-to-end assembly of gold nanorods by biotin-streptavidin connectors. *J*. *Am*. *Chem*. *Soc*. **125**, 13914-13915 (2003).

33. Fu, Y., Zhang, J., & Lakowicz, J. R. Plasmon-enhanced fluorescence from single fluorophores end-linked to gold nanorods. *J*. *Am*. *Chem*. *Soc*. **132**, 5540-5541 (2010).